Research Article

INTERNATIONAL JOURNAL OF ADVANCED ROBOTIC SYSTEMS

International Journal of Advanced Robotic Systems
November-December 2016: 1–13

DOI: 10.1177/1729881416657931
arx.sagepub.com
SAGE

Optimization of potential field method parameters through networks for swarm cooperative manipulation tasks

Rocco Furferi, Roberto Conti, Enrico Meli, and Alessandro Ridolfi

Abstract

An interesting current research field related to autonomous robots is mobile manipulation performed by cooperating robots (in terrestrial, aerial and underwater environments). Focusing on the underwater scenario, cooperative manipulation of Intervention-Autonomous Underwater Vehicles (I-AUVs) is a complex and difficult application compared with the terrestrial or aerial ones because of many technical issues, such as underwater localization and limited communication. A decentralized approach for cooperative mobile manipulation of I-AUVs based on Artificial Neural Networks (ANNs) is proposed in this article. This strategy exploits the potential field method; a multi-layer control structure is developed to manage the coordination of the swarm, the guidance and navigation of I-AUVs and the manipulation task. In the article, this new strategy has been implemented in the simulation environment, simulating the transportation of an object. This object is moved along a desired trajectory in an unknown environment and it is transported by four underwater mobile robots, each one provided with a seven-degrees-of-freedom robotic arm. The simulation results are optimized thanks to the ANNs used for the potentials tuning.

Keywords

Underwater robotics, underwater manipulation, autonomous underwater vehicle, potential field method, artificial neural networks

Date received: 18 January 2016; accepted: 21 May 2016

Topic: Robot Manipulation and Control
Topic Editor: Andrey V Savkin

Introduction

Mobile manipulation performed by cooperating robots, with one or more arms, is for sure a challenging and an open research topic for autonomous robots (Figure 1(a)), especially in relation to an underwater environment.[1–4] Such kinds of systems can have the capability of performing complex tasks that cannot be reached using a single manipulator.

Cooperative manipulation of Intervention-Autonomous Underwater Vehicles (I-AUVs) (Figure 1(b))[5] represents a more complex field of application, compared with the terrestrial or aerial applications, mainly due to different technological problems e.g. localization and communication in underwater environment. However, the use of Autonomous Underwater Vehicles (AUVs) and I-AUVs will necessarily grow up in the future exploration of the sea. In this scenario, cooperative I-AUVs represent the natural evolution of centralized I-AUVs because they may be used in various underwater assembly tasks, such as complex underwater structure construction and maintenance (e.g. underwater pipeline and cable transportation could be carried out by multiple cooperative I-AUVs; underwater search and

Department of Industrial Engineering, University of Florence, Italy

Corresponding author:
Rocco Furferi, Department of Industrial Engineering, University of Florence, Via di Santa Marta, 3 50139 Firenze, Italy.
Email: rocco.furferi@unifi.it

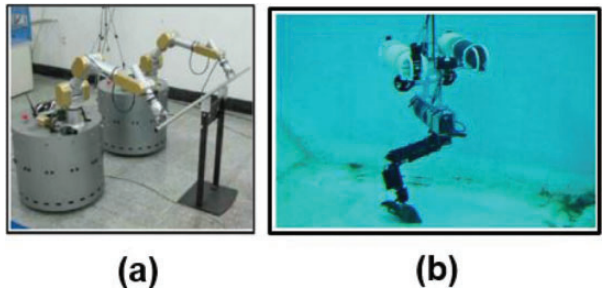

Figure 1. (a) Cooperative mobile manipulation for terrestrial robot. (b) Prototype of intervention-autonomous underwater vehicle.

rescue tasks could be more efficient and effective if multiple I-AUVs could be used[6,7]). In Joordens et al.[1] and Champion et al.,[2] a complete review of the latest cooperative strategies in the underwater field has been described. In Hausler et al.,[8] an interesting method for the optimal motion planning of vehicles is presented.

Usually, the strategies for cooperative mobile manipulation can be addressed dividing the approach into different tasks; these tasks are performed in parallel.

- Swarm motion planning and control: I-AUVs swarm control has been discussed in a few research articles.[9–11] Some effort has been made regarding cooperative localization and communication.[12]
- Vehicle modelling, motion planning and control: Antonelli,[4] Antonelli et al.[13] and Fossen[14] propose models for AUVs and I-AUVs. For example, a tracking control law for a desired I-AUV trajectory is given in Antonelli et al.[13] In Antonelli,[4] the I-AUV model has been partially decoupled and the control scheme compensates the non linear coupling effects.
- Robotic arm motion planning and control: different force control schemes are given in Siciliano et al.,[3] Antonelli[4] and Simetti et al.[5] In Sugar et al.,[15] a solution to the redundancy resolution problem and motion coordination between vehicle and manipulator has been presented using fuzzy techniques.

Most of these approaches present different but independent solutions for swarm, vehicle and robotic arm motion planning and control.

In Sugar et al.,[16] the authors proposed to partially fill this lack in the state of the art through an innovative approach for cooperative mobile manipulation completely based on the potential field method. In fact, the proposed method is based on an innovative decentralized approach for cooperative mobile manipulation of I-AUVs. This strategy is based on a different use of the potential field method (classically used for obstacle avoidance tasks); in particular, a multi-layer control structure is developed to manage in parallel the coordination of the swarm, the guidance and navigation of I-AUVs and the manipulation tasks. The main advantage of the potential field method is the complete integration of all the controller layers within a compact structure. In addition, the amount of information required for the functioning of the control algorithm (distances among all the subjects) is lower than the classical localization strategies. In fact, underwater fleets usually use complex localization algorithms and redundant expensive sensors (e.g. Ultra-Short Base-Line (USBL))[12,17]; the approach proposed in Conti et al.[16] exploited the object to be manipulated (supposed to be partially known) such as a swarm reference system and the surface vehicle only as a connection point with the world reference system. However, in this latter work, the potential field parameters have been tuned through particular numerical simulations in order to obtain sufficiently smooth trajectories for the I-AUVs.

Therefore, in the present article, the authors explore and apply Artificial Neural Network (ANN) techniques to optimize the potential field parameters; ANNs in fact allow the reduction of the simulation time and propose a standard method for parameter optimization (obtained after a training of the neural network).

In conclusion, in this article an innovative cooperative mobile manipulation algorithm based on ANNs for underwater vehicles has been defined. For the testing of the control architecture and the optimization of the potential field method parameters, the Matlab-Simulink simulation environment has been employed. An I-AUV swarm composed of four vehicles, each one provided with a seven-degrees-of-freedom (DOFs) robotic arm, navigates performing the transportation of a known object in an unknown environment (e.g. a harbour); in particular, the manipulation task is to carry the object along a desired trajectory where an obstacle is placed. The article is organized as follows: in the section 'Introduction', a brief introduction of the current issues and possible solutions has been described. In the section 'A new strategy for I-AUVs swarms performing cooperative mobile manipulation', the new cooperative control architecture is described in detail. The section 'Artificial neural network for parameter optimization' proposes the use of ANNs to optimize the potential field parameters to guarantee the best tracking of a suitable trajectory. The sections 'Numerical simulations and results' and 'Conclusions and further developments' summarize the results of the numerical simulations performed to test the algorithm and its pros and cons.

A new strategy for I-AUVs swarms performing cooperative mobile manipulation

This chapter illustrates the control strategy specifically designed for the cooperative mobile manipulation of the I-AUVs swarm. Two main issues are faced: the high-level control of the swarm (including vehicles and robotic

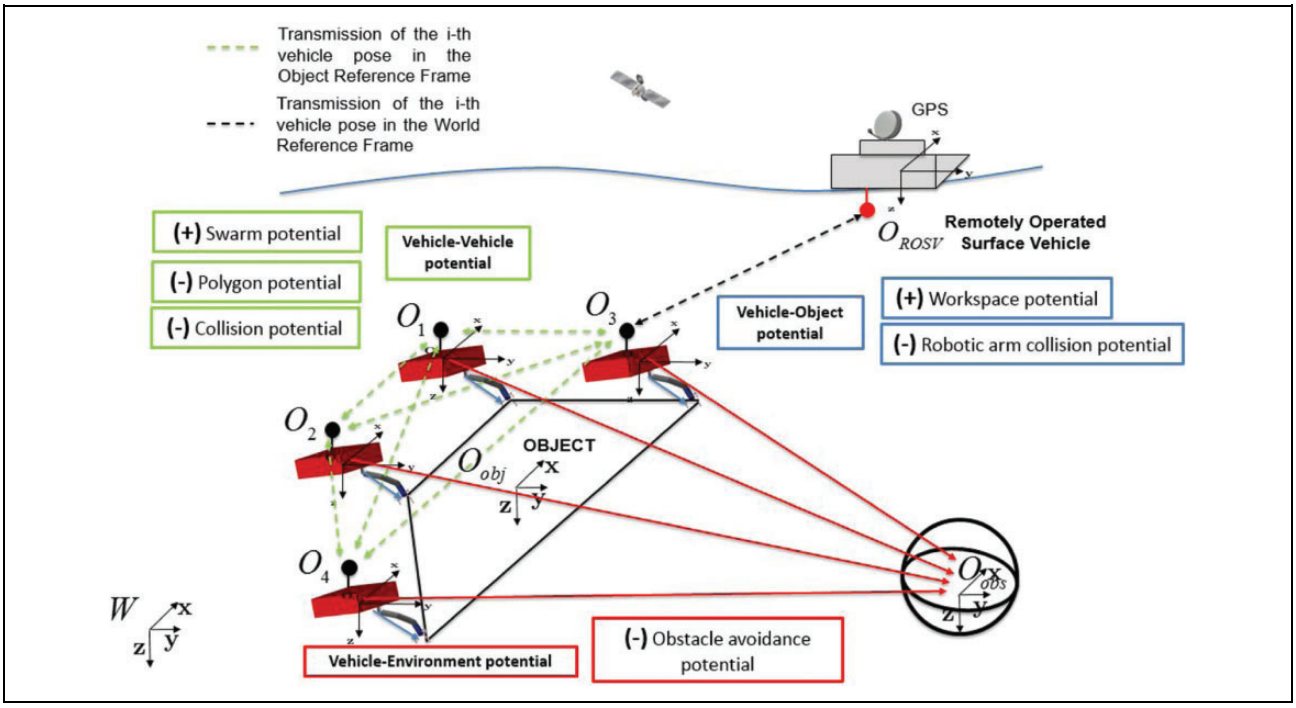

Figure 2. Swarm control architecture: interactions among field potentials. The attractive potentials have the $(+)$, while the repulsive ones have the $(-)$.

arms) and the underwater localization. The I-AUV swarm involves four I-AUVs and an external supporting vehicle (e.g. a Remotely Operated Surface Vehicle (ROSV)). The ROSV geo-localizes the swarm by means of a GPS system and communicates with the I-AUVs through a USBL, transmitting only the position of one of the swarm vehicles in the world reference system. The swarm vehicles share among each other the relative positions in the object reference system through standard acoustic modems. Consequently, the presented approach is completely decentralized and the localization is carried out only by means of few on-board sensors, while the distances among the vehicles are calculated directly in the object reference systems (master vehicles are not required).

The control architecture and the potential field method

Control architectures able to contemporaneously consider guidance of the swarm; vehicles navigation and object manipulation are crucial in cooperative mobile manipulation tasks performed by I-AUVs swarms. To face problems arising from unstructured environments where the vehicle trajectories cannot be generated a priori (for instance in the presence of obstacles[3]), vehicle control strategies based on potential field methods are usually employed, based on the estimation of the vehicle distance vectors. In this article, an innovative control architecture based on the potential field method both to generate the vehicles' trajectory in unstructured environments and to manage manipulation tasks and swarm control during the whole mission has been developed. Since each vehicle exploits only a few on-board sensors, the proposed strategy is completely decentralized from a communication and a localization viewpoint.

According to the potential field method, the I-AUVs are particles immersed in a potential field generated by the goals and by the obstacles. The potential field can be though of as an energy field and its gradient as a force. The goals are surrounded by an attractive potential, while the obstacles are surrounded by a repulsive potential. The vehicles in the potential field perceive two force contributions: the target force (caused by the attractive goal potential field gradient) drives the vehicles to the goals while the obstacle force repulses the vehicles from the obstacles (caused by the repulsive obstacle potential field gradient). Some working hypotheses are needed to develop the control architecture: the object shape and connection points of the vehicles are supposed to be known thanks to suitable acoustic and optical sensors (the gripper–object contact is modelled through a proper kinematic constraint); the I-AUV internal control directly orients the vehicle towards the attractive target direction; finally, the approaching phase to the object is not considered in this analysis. Figure 2 highlights the interactions among vehicles, objects and the environment.

Three different elements play a fundamental role in the control architecture: the vehicles, the object and the environment. Each field potential used in the proposed strategy is related to the interactions among these elements.

1. Vehicle–vehicle (green): the interactions among vehicles comprise two contributions, the first one to maintain the swarm formation and the second one to avoid collisions among the vehicles.

2. Vehicle–environment (red): the interactions between vehicles and environment (obstacle avoidance) are reported in red and the four arrows highlight the single interactions.
3. Vehicle–object (blue): the interactions between vehicles and the object to be manipulated are reported in blue and the four arrows highlight the single connections.

The three field potentials introduced above will be explained in detail in the following sections.

Vehicle–vehicle potential. To build the vehicle–vehicle potential $V_{\mathrm{v-v}}$, three terms are needed: the attractive potential to ensure the swarm formation (for instance to force them into a sphere, useful for this kind of task), the repulsive potential to force the vehicles into a desired shape (as the vertices of regular polygons) and the repulsive potential to prevent vehicles collisions. The potential equations for the i th vehicles (for $i = 1, \ldots, n$ where n is the number of vehicles) can be written as

$$\vec{F}_{\mathrm{v-v},i} = \vec{\nabla} V_{\mathrm{v-v},i} \tag{1}$$

with

$$V_{\mathrm{v-v},i} = V_i^{\mathrm{swarm}} + V_{i,j}^{\mathrm{polygon}} + V_{i,j}^{\mathrm{collisions}} \tag{2}$$

where $V_{\mathrm{v-v},i}$ is the overall vehicle–vehicle potential acting on the i th vehicle (for $i = 1, \ldots, n$), V_i^{swarm} is the formation potential, $V_{i,j}^{\mathrm{polygon}}$ is the shape potential (where $j = 1, \ldots, n$ and $j \neq i$) and $V_{i,j}^{\mathrm{collisions}}$ is the collision potential (where $j = 1, \ldots n$ and $j \neq i$). The formation potential is employed both to maintain the I-AUVs in a sphere and to lead the vehicles towards the target. In this circumstance, the vector $\vec{d}_i^{\,\mathrm{W}} = \vec{\eta}_i^{\,\mathrm{W}} - \vec{G}_{\mathrm{d}}^{\,\mathrm{W}}(t)$ (written in the world reference system, specified by the pedix $^{\mathrm{W}}$) is the distance between the vehicle position $\vec{\eta}_i^{\,\mathrm{W}}$ and the sphere centre $\vec{G}_{\mathrm{d}}^{\,\mathrm{W}}(t)$ (the swarm trajectory to be tracked). Consequently, the force $\vec{F}_i^{\mathrm{swarm}}$ acting on the I-AUV is

$$\vec{F}_i^{\mathrm{swarm}} = \vec{\nabla} V^{\mathrm{swarm}} = -f^{\mathrm{swarm}}\left(\left\|\vec{d}_i^{\,\mathrm{W}}\right\|\right) \frac{\left(\vec{\eta}_i^{\,\mathrm{W}} - \vec{G}_{\mathrm{d}}^{\,\mathrm{W}}(t)\right)}{\left\|\vec{\eta}_i^{\,\mathrm{W}} - \vec{G}_{\mathrm{d}}^{\,\mathrm{W}}(t)\right\|} \tag{3}$$

where $f^{\mathrm{swarm}}\left(\left\|\vec{d}_i^{\,\mathrm{W}}\right\|\right)$ depends on the distance. This function introduces a low boundary (equal to the radius R of the sphere) to attract the vehicle lying outside the shape and to keep free the vehicles inside: $f^{\mathrm{swarm}}\left(\left\|\vec{d}_i^{\,\mathrm{W}}\right\|\right) = k_{\mathrm{s}}\left(\left\|\vec{d}_i^{\,\mathrm{W}}\right\| - R\right)^2$ for $\left\|\vec{d}_i^{\,\mathrm{W}}\right\| \geq R$ and 0 outside, where k_{s} is the parameter that increases the curve slope.

The shape potential V^{polygon} is repulsive and aims at pushing the vehicles towards the vertices of a regular polygon on the sphere surface (the specific polygon depends on the number of vehicles). In this kind of potential, the key physical quantity is the inverse of the distance between two vehicles $\vec{d}_{i,j}^{\,\mathrm{W}} = \vec{\eta}_i^{\,\mathrm{W}}(t) - \vec{\eta}_j^{\,\mathrm{W}}(t)$ where $\vec{\eta}_i^{\,\mathrm{W}}$, $\vec{\eta}_j^{\,\mathrm{W}}$ are respectively the i th and j th vehicle positions (for $j \neq i$). Consequently, the force $\vec{F}_{i,j}^{\mathrm{polygon}}$ acting on the i th vehicle is the sum of the contributions related to each vehicle

$$\vec{F}_{i,j}^{\mathrm{polygon}} = \vec{\nabla} V_{i,j}^{\mathrm{polygon}} = f^{\mathrm{polygon}}\left(\left\|\vec{d}_{i,j}^{\,\mathrm{W}}\right\|\right) \frac{\left(\vec{\eta}_i^{\,\mathrm{W}}(t) - \vec{\eta}_j^{\,\mathrm{W}}(t)\right)}{\left\|\vec{\eta}_i^{\,\mathrm{W}}(t) - \vec{\eta}_j^{\,\mathrm{W}}(t)\right\|} \tag{4}$$

where $f^{\mathrm{polygon}}\left(\left\|\vec{d}_{i,j}^{\,\mathrm{W}}\right\|\right)$ always depends on the distance. This repulsive function introduces an upper bound (equal to the diameter of the sphere) to push the vehicles on the surface: $f^{\mathrm{polygon}}\left(\left\|\vec{d}_{i,j}^{\,\mathrm{W}}\right\|\right) = k_{\mathrm{p}}\left(\frac{1}{\left\|\vec{d}_{i,j}^{\,\mathrm{W}}\right\|^2} - \frac{1}{4R^2}\right)$ for $\left\|\vec{d}_i^{\,\mathrm{W}}\right\| < 2R$ and 0 outside, where k_{p} is again the parameter controlling the curve slope: thanks to this potential, the vehicles will be pushed towards the vertices of a regular polygon (depending on the number of vehicles).

Eventually, the collision potential $V_{i,j}^{\mathrm{collisions}}$ is repulsive as well and must avoid collisions among the vehicles. The potential is useful especially when the transported object is small in comparison with the vehicle dimensions and the risk of vehicle collisions is high. Also in this last case, the key physical quantity is the inverse of the distance among two vehicles $\vec{d}_{i,j}^{\,\mathrm{W}} = \vec{\eta}_i^{\,\mathrm{W}}(t) - \vec{\eta}_j^{\,\mathrm{W}}(t)$ described before. Analogously, the force $\vec{F}_{i,j}^{\mathrm{collisions}}$ acting on the i th vehicle is the sum of the contributions related to each vehicle

$$\begin{aligned}\vec{F}_{i,j}^{\mathrm{collisions}} &= \vec{\nabla} V_{i,j}^{\mathrm{collisions}} \\ &= f^{\mathrm{collisions}}\left(\left\|\vec{d}_{i,j}^{\,\mathrm{W}}\right\|\right) \frac{\left(\vec{\eta}_i^{\,\mathrm{W}}(t) - \vec{\eta}_j^{\,\mathrm{W}}(t)\right)}{\left\|\vec{\eta}_i^{\,\mathrm{W}}(t) - \vec{\eta}_j^{\,\mathrm{W}}(t)\right\|}\end{aligned} \tag{5}$$

where $f^{\mathrm{collisions}}\left(\left\|\vec{d}_{i,j}^{\,\mathrm{W}}\right\|\right)$ depends on the distance. This function introduces an upper bound equal, in this case, to the double of the vehicle sizes. This approximation allows the avoidance of vehicle collisions: $f^{\mathrm{collisions}}\left(\left\|\vec{d}_{i,j}^{\,\mathrm{W}}\right\|\right) = k_{\mathrm{c}}\left(\frac{1}{\left\|\vec{d}_{i,j}^{\,\mathrm{W}}\right\|^2} - \frac{1}{d_{\mathrm{c}}^2}\right)$ for $\left\|\vec{d}_i^{\,\mathrm{W}}\right\| < d_{\mathrm{c}}$ and 0 outside, where k_{c} is, as usual, the parameter governing the curve slope and d_{c} is a safety distance, for example the double of the vehicle sizes.

Vehicle–object potential. The vehicle–object potential $V_{\mathrm{v-o}}$ allows the right position of the end-effector to be kept with respect to the I-AUV position. In more detail, the potential is built through a function of the end-effector–vehicle distance ($d_{\mathrm{ee,v}}^{\mathrm{W}}$) composed of three parts: the first zone ($0 \leq d_{\mathrm{ee,v}}^{\mathrm{W}} < WS_{\mathrm{min}}$) is repulsive to avoid end-effector–vehicle collisions; in the second zone ($WS_{\mathrm{min}} \leq d_{\mathrm{ee,v}}^{\mathrm{W}} < WS_{\mathrm{max}}$), the potential is not active because, in this

zone, the standard kinematic controls are exploited; finally, in the third zone ($d^{\mathrm{W}}_{\mathrm{ee,v}} \geq WS_{\max}$), the potential is attractive to push the I-AUV towards the workspace of the robotic arm. In this application, the vehicle–object potential acts directly on the vehicle motion to better exploit the motor thrusts. The use of suitable potentials instead of classical kinematic controls allows reduction of the stiffness of the systems and the dynamic interactions between vehicles and robotic arms.

The vehicle–object potential comprises two functions: the workspace potential V^{WS} and the robotic arm collision potential V^{RAcoll}

$$V_{\mathrm{v-o}} = V^{\mathrm{WS}} + V^{\mathrm{RAcoll}} \tag{6}$$

where $V_{\mathrm{v-o}}$ is the overall vehicle–object potential, V^{WS} is the workspace potential, allowing the end-effector position to be kept in the workspace of the robotic arm, and V^{RAcoll} is the robotic arm collision potential to prevent vehicle–end-effector collisions. Note that $d^{\mathrm{W}}_{\mathrm{ee,v}} = \left\|\vec{\eta}^{\,\mathrm{W}}_{v} - \vec{\eta}^{\,\mathrm{W}}_{\mathrm{ee}}\right\|$ is the distance between robotic arm $\vec{\eta}^{\,\mathrm{W}}_{v}$ and end-effector $\vec{\eta}^{\,\mathrm{W}}_{\mathrm{ee}}$

$$\vec{F}^{\,\mathrm{WS}} = \vec{\nabla} V^{\mathrm{WS}} = -f^{\mathrm{WS}}\left(\left\|\vec{d}^{\,\mathrm{W}}_{\mathrm{ee,v}}\right\|\right)\frac{(\vec{\eta}^{\,\mathrm{W}}_{v} - \vec{\eta}^{\,\mathrm{W}}_{\mathrm{ee}})}{\left\|\vec{\eta}^{\,\mathrm{W}}_{v} - \vec{\eta}^{\,\mathrm{W}}_{\mathrm{ee}}\right\|} \tag{7}$$

where $f^{\mathrm{WS}}\left(\left\|\vec{d}^{\,\mathrm{W}}_{\mathrm{ee,v}}\right\|\right) = -k_{\mathrm{WS}}\left(\left\|\vec{d}^{\,\mathrm{W}}_{\mathrm{ee,v}}\right\| - WS_{\max}\right)^2$ depends on the distance for $\left\|\vec{d}^{\,\mathrm{W}}_{\mathrm{ee,v}}\right\| < WS_{\max}$ and 0 outside, k_{WS} is the standard parameter governing the curve slope and $WS_{\max}$ is the robotic arm maximum extension.

On the contrary, the robotic arm collision potential is repulsive and has to maintain the end-effector away from the I-AUV. The key distance to be taken into account is again: $d^{\mathrm{W}}_{\mathrm{ee,v}} = \left\|\vec{\eta}^{\,\mathrm{W}}_{v} - \vec{\eta}^{\,\mathrm{W}}_{\mathrm{ee}}\right\|$ while the force $\vec{F}^{\,\mathrm{RAcoll}}$ on the I-AUV can be written as

$$\vec{F}^{\,\mathrm{RAcoll}} = \vec{\nabla} V^{\mathrm{RAcoll}} = f^{\mathrm{RAcoll}}\left(\left\|d^{\mathrm{W}}_{\mathrm{ee,v}}\right\|\right)\frac{(\vec{\eta}^{\,\mathrm{W}}_{v} - \vec{\eta}^{\,\mathrm{W}}_{\mathrm{ee}})}{\left\|\vec{\eta}^{\,\mathrm{W}}_{v} - \vec{\eta}^{\,\mathrm{W}}_{\mathrm{ee}}\right\|} \tag{8}$$

where $f^{\mathrm{RAcoll}}\left(\left\|\vec{d}^{\,\mathrm{W}}_{\mathrm{ee,v}}\right\|\right)$ depends as usual on the distance. The repulsive potential is characterized by an upper bound equal to the robotic arm minimum extension: $f^{\mathrm{RAcoll}}\left(\left\|\vec{d}^{\,\mathrm{W}}_{\mathrm{ee,v}}\right\|\right) = k_{\mathrm{RA}}\left(\frac{1}{\left\|\vec{d}^{\,\mathrm{W}}_{\mathrm{ee,v}}\right\|^2} - \frac{1}{WS^2_{\min}}\right)$ for $\left\|\vec{d}^{\,\mathrm{W}}_{\mathrm{ee,v}}\right\| < WS_{\min}$ and 0 outside, in which k_{RA} governs the curve slope and $WS_{\min}$ is the robotic arm minimum extension. If needed, both these parts can be exploited to avoid robotic arm–vehicle collisions as well.

Vehicle–environment potential. To manage obstacle avoidance during the object transportation, a repulsive vehicle–environment potential $V_{\mathrm{v-e}}$ is required.

The vehicle–environment potential $V_{\mathrm{v-e}}$ is built for each obstacle. The key physical quantity to be taken into account is the inverse of the vehicle–obstacle distance $d^{\mathrm{W}}_{i,o} = \left\|\vec{\eta}_i^{\,\mathrm{W}}(t) - \vec{\eta}^{\,\mathrm{W}}_{\mathrm{o}}, (t)\right\|$ where $\vec{\eta}_i^{\,\mathrm{W}}$ is the i th vehicle position and $\vec{\eta}_{\mathrm{o}}$, is the obstacle position. At this point, the force $\vec{F}^{\,\mathrm{v-e}}_{i,o}$ on the i th vehicle can be written as

$$\vec{F}^{\,\mathrm{v-e}}_{i,o} = \nabla V_{\mathrm{v-e}} = +f^{\mathrm{v-e}}_{\iota,\mathrm{o}}\left(\left\|\vec{d}^{\,\mathrm{W}}_{\iota,\mathrm{o}}\right\|\right)\frac{(\vec{\eta}^{\,\mathrm{W}}_{\iota}(t) - \vec{\eta}^{\,\mathrm{W}}_{\mathrm{o}}, (t))}{\left\|\vec{\eta}^{\,\mathrm{W}}_{\iota}(t) - \vec{\eta}^{\,\mathrm{W}}_{\mathrm{o}}, (t)\right\|} \tag{9}$$

where $f^{\mathrm{v-e}}_{i,o}\left(\left\|\vec{d}^{\,\mathrm{W}}_{i,o}\right\|\right)$ depends as usual on the distance. This repulsive potential introduces an upper bound equal to a safety distance e.g. the double of the vehicle size d_{O}, to avoid the obstacle. The potential is defined as $f^{\mathrm{v-e}}_{i,o}\left(\left\|\vec{d}^{\,\mathrm{W}}_{i,o}\right\|\right) = k_{\mathrm{O}}\left(\frac{1}{\left\|\vec{d}^{\,\mathrm{W}}_{i,o}\right\|^2} - \frac{1}{d^2_{\mathrm{O}}}\right)$ and 0 outside, in which k_{O} is again the curve slope parameter.

Distance estimation algorithm

Underwater swarm localization is usually based on expensive sensors, such as long base-line or USBL, able to provide the proper position of each vehicle in the world reference frame.[12,17] The main drawback of the current approaches is mainly related to the low frequency of the vehicle position update: this is hardly acceptable for cooperative manipulation tasks because the position update at a higher frequency is important to obtain correct control actions. In particular, the proposed control architecture for the maintaining of the swarm formation and the execution of cooperative manipulation tasks, exploiting the potential field method, requires a constant distance vectors update. Therefore, in the present article, an innovative localization strategy has been developed. On-board sensors (e.g. inertial measurement unit (IMU), cameras, echo-sounder) with a high-frequency rate are considered to overcome this issue: these sensors firstly provide the vehicle position with respect to the object reference frame and then the reciprocal distances of the vehicles. A completely decentralized solution is given to perform the cooperative manipulation task, uniquely based on distance vector estimations (Table 1).

First, it is useful to define some physical quantities and the reference frames involved in the estimation algorithm (used by every vehicle to calculate its potentials). $\vec{\eta}^{\,\mathrm{W}}_{\mathrm{v}i}$, is the i th vehicle position, $\vec{G}^{\,\mathrm{W}}_{\mathrm{d}}(t)$ is the central position of the swarm circle, $\vec{\eta}^{\,\mathrm{W}}_{\mathrm{ee},i}$ is the position of the i th vehicle end-effector and $\vec{\eta}^{\,\mathrm{W}}_{\mathrm{o}}$ is the central position of the obstacle. All these vectors are given in the world reference frame.

The proposed approach reduces the data exchange between underwater vehicles and the ROSV to increase the reliability of the control architecture. The manipulated object is a local reference system of the swarm. Through the hypotheses of known object and known connection points between I-AUVs and objects, the distance vectors can be easily determined; on-board sensors, e.g. cameras, IMU, joint sensors with high data-flow rates, provide the correct position of the I-AUV in the object reference frame.

Table 1. Distance vectors.

NÂ°	Distance vector	Potential functions	Equation
I	Distance between I-AUVs	$V_i^{\text{collisions}}$-V^{polygon}	$\vec{d}_{i,j}^{\,\text{W}} = (\vec{\eta}_{\text{vi}}^{\,\text{W}}, (t) - \vec{\eta}_{\text{vj}}^{\,\text{W}}(t)) = R_{\text{IMU}}^{Ti} R_{\text{DK}i}^{\text{T}} \vec{d}_{i,j}^{\,\text{obj}}$
II	Distance between I-AUVs and the swarm sphere	V^{swarm}	$\vec{d}_i^{\,\text{W}} = (\vec{\eta}_{\text{vi}}^{\,\text{W}}, -\vec{G}_{\text{d}}^{\,\text{W}}(t))$
III	Distance between I-AUV(i th) and end-effector(i th)	V^{WS}-V^{RAcoll}	$\vec{d}_{\text{ee,v}}^{\,\text{W}} = (\vec{\eta}_{\text{vi}}^{\,\text{W}}, -\vec{\eta}_{\text{ee}}^{\,\text{W}}) = R_{\text{IMU}}^{i}(\vec{d}_{v,i}^{\,V} + \vec{d}_{\text{DK}i}^{\,V})$
IV	Distance between i th vehicle and obstacle	$V_{\text{v}-\text{e}}$	$\vec{d}_{i,o}^{\,\text{W}} = (\vec{\eta}_i^{\,\text{W}}(t) - \vec{\eta}_{\text{o}}^{\,\text{W}}, (t)) = R_{\text{IMU}}^{i} \vec{d}_{\text{obs}}, ^{V}$

A world reference frame $\vec{O}_{\text{W}}$, an i th vehicle reference frame $\vec{O}_{\text{v}i}$, and an object reference frame $\vec{O}_{\text{obj}}$ are defined. R_{IMU}^{i} and $R_{\text{DK}i}$, are the rotation matrices respectively between $\vec{O}_{\text{W}}$ and $\vec{O}_{\text{v}i}$, and between $\vec{O}_{\text{v}i}$, and $\vec{O}_{\text{obj}}$. R_{IMU}^{i} can be obtained only through an on-board IMU for the vehicle orientation measurements (e.g. providing the Euler angles, e.g. ϕ_V,θ_V,ψ_V), and $R_{\text{DK}i}$ is calculated from the robotic arm direct kinematic model. The distance vectors given in Table 1 with respect to the world reference frame can be rewritten in the vehicle reference frame.

1. Ist distance (the distance among vehicles $\vec{d}_{i,j}^{\,\text{W}}$): rewriting the position of the i th vehicle in the object reference frame $O_{\text{obj}}^{\text{W}}$, it is possible to obtain

$$\vec{\eta}_{\text{OV}i}^{\,\text{obj}} = \vec{d}_{\text{cp}}^{\,\text{obj},i} + R_{\text{DK}i}\vec{d}_{\text{DK}i}^{\,\text{V}} + R_{\text{DK},i}\vec{d}_{\text{V}}^{\,\text{V},i} \tag{10}$$

where $\vec{d}_{cp}^{\,obj,i}$ is the known position of the connection point in the object reference frame, $\vec{d}_{\text{DK}i}^{\,V}$ is the end-effector position in the manipulator base reference frame and $\vec{d}_{V}^{\,V,i}$ is the position of the manipulator base in the vehicle reference frame (a priori known). The position of the vehicles, in the object reference frame, can be calculated through equation (10); the distance vectors $\vec{d}_{i,j}^{\,\text{obj}}$ are

$$\vec{d}_{i,j}^{\,\text{obj}} = \vec{\eta}_{\text{OV}i}^{\,\text{obj}} - \vec{\eta}_{\text{OV}j}^{\,\text{obj}} \tag{11}$$

expressed in the world reference frame as

$$\vec{d}_{i,j}^{\,\text{W}} = R_{\text{IMU}}^{Ti} R_{\text{DK}i}^{\text{T}} \vec{d}_{i,j}^{\,\text{obj}} \tag{12}$$

Equation (12) is completely decentralized because the positions of other I-AUVs are based on on-board data and local vehicle positions in the object reference frame (transmitted by means of acoustic modems). The I-AUVs' positions in the object reference frame $\vec{\eta}_{\text{OV}i}^{\,\text{obj}}$, for $i = 1, 2, \ldots, n_{\text{vei}}$ with n_{vei} number of vehicles, transmitted among the vehicles through underwater acoustic modems.

2. IInd distance (distance between I-AUVs and the swarm sphere $\vec{d}_i^{\,\text{W}}$): this distance cannot be calculated into the vehicle reference frame. Every vehicle finds its position in the world reference frame. The algorithm exploits the distance calculated in the previous step $\vec{d}_{i,j}^{\,\text{W}}$ and the position in the world reference frame of one vehicle of the swarm; the i th vehicle can recalculate the other vehicle positions ($j \neq i$) in the world reference frame by summing its position in the world reference frame and the distance vector for each vehicle (equation (13)). As regards the position in the world reference frame, the algorithm needs an I-AUV (one of the swarm) to receive its position $\vec{\eta}_{\text{v}i}^{\,\text{W}}$ (provided by the ROSV) and this info will be transmitted to the other vehicles of the swarm.

$$\vec{\eta}_{\text{v}j}^{\,\text{W}} = \vec{\eta}_{\text{v}i}^{\,\text{W}} + \vec{d}_{i,j}^{\,\text{W}} \quad j \neq i, \ \text{for} j = 1, 2, \ldots, n_{\text{vei}} \tag{13}$$

The central position of the swarm $\vec{G}_{\text{d}}^{\,\text{W}}(t)$ is the desired position transmitted through acoustic modems. This data is obtained by equation (14), with a relatively low time rate

$$\vec{G}_{\text{d}}^{\,\text{W}}(t) = \vec{\eta}_{\text{ROSV}}^{\,\text{W}} + \vec{G}_{d-\text{ROSV}}^{\,\text{W}}(t) \tag{14}$$

where $\vec{\eta}_{\text{ROSV}}^{\,\text{W}}$ is the ROSV world position acquired by the GPS and $\vec{G}_{d-\text{ROSV}}^{\,\text{W}}(t)$ is the desired position of the swarm with respect to the ROSV. Therefore, $\vec{d}_i^{\,\text{W}}$ is obtained as $\vec{\eta}_{\text{v}i}^{\,\text{W}} - \vec{G}_{\text{d}}^{\,\text{W}}(t)$.

3. IIIrd distance (distance between the i th vehicle and the i th end-effector $\vec{d}_{\text{ee,v}}^{\,\text{W}}$): it can be easily computed in the world reference frame from equation (15)

$$\vec{d}_{\text{ee,v}}^{\,\text{W}} = R_{\text{IMU}}^{i}(\vec{d}_{v,i}^{\,V} + \vec{d}_{\text{DK}i}^{\,V}) \tag{15}$$

where $\vec{d}_{v,i}^{\,V}$ is the distance of the manipulator base into the vehicle reference frame, R_{IMU}^{i} is the rotation matrix between world and vehicle reference frames and $\vec{d}_{\text{DK}i}^{\,V}$ is the distance vector due to the direct kinematics.

1. IVth distance (distance between the i th vehicle and the obstacle $\vec{d}_{i,\text{o}}^{\,\text{W}}$): it can be computed in the vehicle reference frame. The value $\vec{d}_{\text{obs}}^{\,V}$ comes from the on-board sensors (e.g. optical cameras or acoustic sensors) and can be easily calculated in the world reference frame (equation (16)) using the rotation matrix between world and vehicle reference frames R_{IMU}^{i}

$$\vec{d}_{i,\text{o}}^{\,\text{W}} = R_{\text{IMU}}^{i}\vec{d}_{\text{obs}}^{\,V} \tag{16}$$

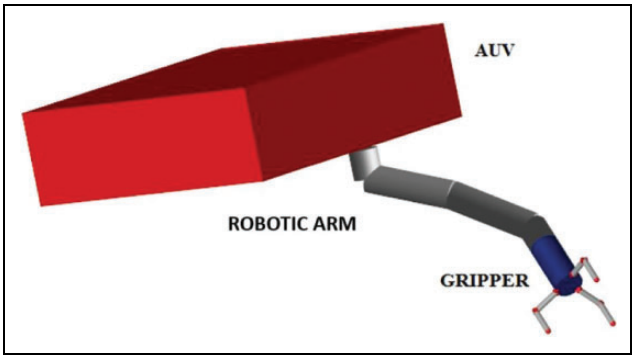

Figure 3. Model of the intervention-autonomous underwater vehicle.

Multibody modelling of the I-AUV

The swarm of I-AUVs comprises n vehicles equipped with a seven-DOFs robotic arm. A specific multibody model of the I-AUV is built, considering both the vehicle and the robotic arm (Figure 3).

The I-AUV geometrical and physical characteristics can be found in the literature and in the related datasheets.[18] Concerning the gripper, it has been assumed to be a rigid gripper-object connection to simplify the model. All the multibody models are assembled using the Matlab-Simulink software.

agreement with the SNAME notation[14], the AUV kinematics is described using the vectors $\vec{\eta}$ and $\vec{\nu}$ where $\vec{\eta} = (\vec{\eta}_1{}^{\mathrm{T}}, \vec{\eta}_2{}^{\mathrm{T}})^{\mathrm{T}}$ contains the position $(\vec{\eta}_1)$ and the orientation $(\vec{\eta}_2)$ in the fixed reference system $< n >$ and $\vec{\nu} = (\vec{\nu}_1^{\mathrm{T}}, \vec{\nu}_2^{\mathrm{T}})^{\mathrm{T}}$ are the linear $(\vec{\nu}_1)$ and the angular $(\vec{\nu}_2)$ velocities in the body reference system $< b >$ (both the reference systems use the standard North-East-Down (NED) directions).

At this point, the vehicle dynamics can be written as[14]

$$M_{\mathrm{RB}}\dot{\vec{\nu}} + C_{\mathrm{RB}}(\vec{\nu})\vec{\nu} = \vec{\tau}_{\mathrm{H}}(\vec{\nu}, \vec{\nu}_C) + \vec{g}(\vec{\eta}) + \vec{\tau} + \vec{\tau}_{\mathrm{g}} \quad (17)$$

in which M_{RB} is the vehicle mass matrix and $C_{\mathrm{RB}}(\vec{\nu})$ is the matrix describing the Coriolis and centrifugal effects. $\vec{g}(\vec{\eta})$, $\vec{\tau}$ and $\vec{\tau}_{\mathrm{g}}$ are the gravity vector, the generalized actions of the vehicle thrusters and the generalized actions caused by the dynamical robotic arm–vehicle interaction, respectively. The main vehicle geometrical and physical data are taken from the literature [18]: DOFs = 6, length $l_{\mathrm{v}} = \approx 0.8$ m, breadth $b_{\mathrm{v}} = \approx 0.6$ m, height $h_{\mathrm{v}} = \approx 0.4$ m and mass $m_{\mathrm{v}} = \approx 150$ kg. The I-AUV is provided with a robotic arm with seven DOFs. The robotic arm is placed on the vehicle bow, in the middle of its lower part. For the kinematic model of the robotic arm (Figure 4), the joint coordinates $\vec{q} = [q_1\, q_2\, \ldots\, q_7]^{\mathrm{T}}$ and the end-effector position $\vec{x} = [x\, y\, z\, \phi\, \theta\, \psi]^{\mathrm{T}}$ are defined. In Figure 4 and Table 2, the Denavit–Hartenberg parameters of the arm are given.

Redundant DOFs can be used to achieve secondary tasks (i.e. the minimization of kinetic energy).[3]

The dynamic model of the robotic arm is simulated and every rigid body is modelled as follows

$$M_l^i\dot{\vec{\nu}}_1^i + C_l^i(\vec{\nu}_1^i)\vec{\nu}_1^i = \vec{\tau}_{\mathrm{H}}^i(\vec{\nu}_1^i, \vec{\nu}_{l\mathrm{C}}^i) + \vec{g}^i(\vec{\eta}_1^i) + \vec{\tau}_{\mathrm{gl}}^i \quad (18)$$

where M_1^i represents the mass matrix, $C_1^i(\vec{\nu}_1^i)$ is the Coriolis and centrifugal effect matrix of the i th link. $\vec{g}^i(\vec{\eta}_1^i)$ and $\vec{\tau}_{\mathrm{gl}}^i$ are respectively the contributions related to the gravity effects and the generalized forces due to the interaction with the other links of the robotic arm. The robotic arm characteristics come from the technical literature[18] and can be synthesized into the following parameters: $d_1 = d_3 = d_5 = d_7 = 0.3$ m are the lengths of the links, $d_1 = 0.2$ m is the link diameter and $m_1 \approx 10$ kg is the link mass.

The hydrodynamics and buoyancy effects $\vec{\tau}_{\mathrm{H}}(\vec{\nu}_{\mathrm{r}}, \vec{\nu}_{\mathrm{C}})$ for the vehicle and for the robotic arm have been considered to reproduce in the I-AUV dynamics during the navigation and manipulation tasks.

The I-AUV control architecture is based on a multilayer approach where the contributions of the different potentials are combined with the classical control techniques. The vehicle can be controlled using different strategies: position control on the six DOFs using the Proportional-Integral-Derivative (PID) approach or force control using the potential approach (on the x–y–z directions). The first approach can be useful for the approaching phase of the I-AUV to the object (precise positioning). The second one merges the control on the x–y–z directions in terms of forces with a PID strategy in terms of angular quantities during cooperative manipulation tasks. Using a suitable matrix H, describing the relations $\vec{\tau} = H\vec{S}$ between vehicle forces $\vec{\tau}$ and thrusts $\vec{S}$[14], the generalized thrusts actions can be evaluated starting from the forces calculated through the field potentials in the vehicle reference systems.

Looking at the robotic arm, the required values of the joints variables (to obtain the desired end-effector position) must be found. To reach this goal, a constrained optimization approach is used. If the required end-effector velocity $\vec{v}_{\mathrm{e}}$ and the Jacobian J are supposed to be known, the solutions $\dot{\vec{q}}_{\mathrm{d}}$ of the linear equation between the end-effector velocity and the joint velocities that minimize the quadratic cost functional of the joint velocities can be found.

Artificial neural network for parameter optimization

As explained above, different swarm trajectories can be followed by the I-AUVs depending on different settings of the vehicle–vehicle, vehicle–object and vehicle–environment potentials. Let, accordingly, P_i be a vector whose elements are the 10 parameters to be set used for a given i th simulation, parameters defined in the section 'A new

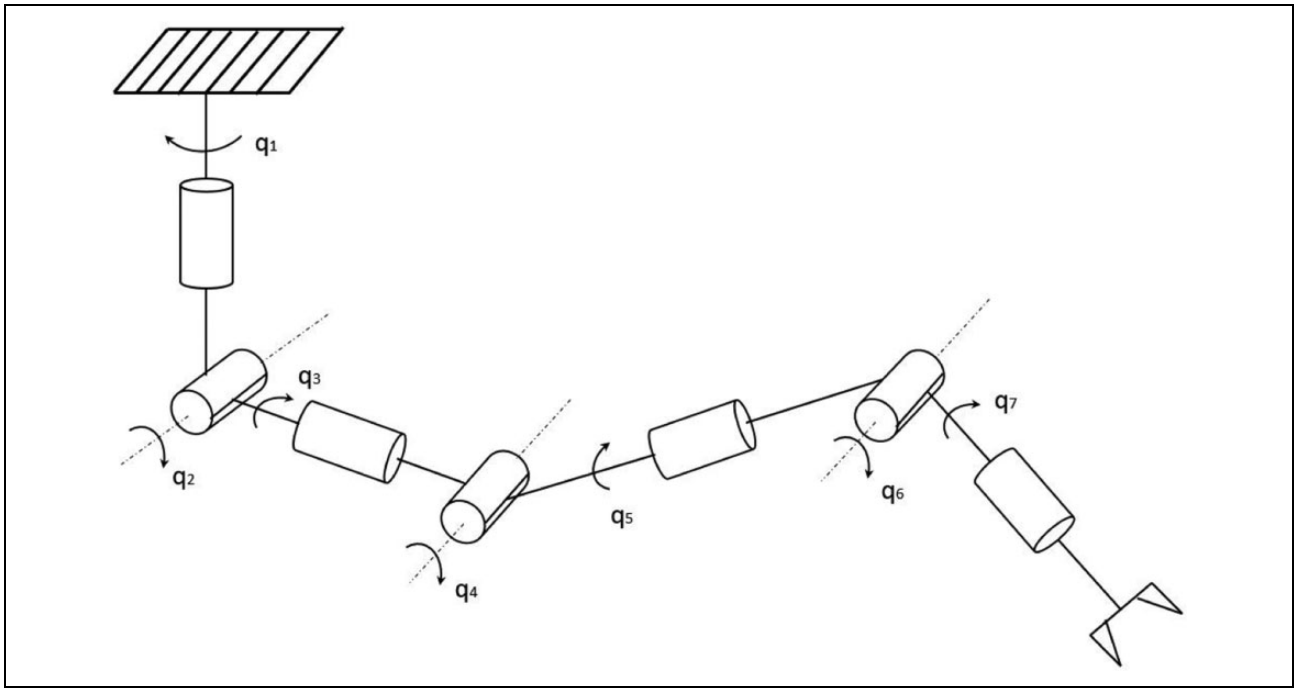

Figure 4. Kinematic scheme of the robotic arm.

Table 2. Robotic arm Denavit–Hartenberg parameters.

Link	a_i	α_i	d_i	ϑ_i
	0	$\pi/2$	d_1	ϑ_1
	0	$\pi/2$	0	$\vartheta_2 + \frac{\pi}{2}$
	0	$-\pi/2$	d_3	ϑ_3
	0	$\pi/2$	0	$\vartheta_4 + \frac{\pi}{2}$
	0	$-\pi/2$	d_5	ϑ_5
	0	$\pi/2$	0	ϑ_6
	0	0	d_7	ϑ_7

strategy for I-AUVs swarms performing cooperative mobile manipulation'

$$\vec{P}_i = (R, k_s, k_p, d_c, k_c, \text{WS}, k_{\text{WS}}, k_{\text{RA}}, d_O, k_O) \quad (19)$$

The resulting desired trajectory, computed using the approach described above, consists of a polyline T_i. Since different values lead to different results, a method to provide the vector P_{opt} able to define the optimal trajectory for safely avoiding the obstacle, is required. To find such a vector, that is, to define the optimal parameters values, a good option could be to apply any optimization algorithms available in literature.[19,20]

In effect, for a given set of these parameters it is possible to simulate the whole trajectory; consequently, it is straightforward to build a dataset of different trajectories by testing different values, varying them within a given range. Unfortunately, since each simulation requires the setting of 10 input parameters, performing a full factorial experiment[21] is not recommended, even in case only two states are selected for each parameter (such an experiment would require $2^{10} = 1024$ simulations to be achieved, involving more than 500 hours of computational time). Obviously, for higher numbers of states, suggested for determining more reliable values, the required experiments increase accordingly thus making impracticable the experimentation.

To overcome this issue, ANNs could be a valid option to infer step-by-step variations of the 10 inputs (within proper ranges) with the swarm actual trajectory by using a lower number of simulations.

As widely recognized[22] artificial neural networks are computational systems that simulate the microstructure of a biological nervous system. ANNs can be trained to perform a particular function either from the information from outside the network or by the neurons themselves in response to the input.[23] A properly trained ANN is capable of generalizing the information on the basis of the parameters acquired during its training phase; as a consequence, for any given input different from the ones used for training, it provides a reliable forecast of the inferred output.

Therefore, in the present work an ANN is built with the aim of finding a transfer function between a given set of values P_i and the resulting trajectory T_i. To reduce the complexity of the devised system, instead of using the whole polyline T_i obtainable from the i th simulation, a parameter l_i describing the lateral offset of the transported object centre of gravity with respect to the obstacle centre is used as target for the ANN.

Accordingly, the ANN, devised by using the Matlab Neural Network Toolbox, is built using the following data.

Table 3. Parameters used for simulating the artificial neural network and allowed values.

Parameter	Allowed values				Step	Units
R	4	4.5	5	5.5	0.5	m
k_s	7	8	9	10	1	N/m^2
k_P	0.08	0.1	0.12	0.14	0.02	Nm^2
d_c	1	1.5	2	2.5	0.5	m
k_c	0.9	1.2	1.5	1.8	0.3	Nm^2
WS	0.4	0.6	0.8	1	0.2	N/m^2
k_{ws}	80	100	120	140	20	Nm^2
k_{RA}	80	100	120	140	20	Nm^2
d_O	15	16	17	18	1	m
k_O	7	8	9	10	1	Nm^2

- The training set consists of a matrix $\vec{P}$ built by choosing 80 different P_i vectors obtained by varying the potentials within the ranges described in Table 3

$$\vec{P} = [P_1, P_2, \ldots, P_{80}] \tag{20}$$

- The target set consists of the vector $\vec{L}$ whose elements are the parameters l_i

$$\vec{L} = [l_1, l_2, \ldots, l_{80}] \tag{21}$$

The ANN architecture is characterized by the following parameters:

- three layers: input, hidden and output layer[22];
- a hidden layer made of logistic neurons followed by an output layer of linear neurons;
- ten input, h hidden, and 1 output units. The number of hidden units was varied from 6 to 18 with a step of 3 units, monitoring the performance of the response using the training data. The number of hidden units that achieved the optimal response is $h = 15$.

The ANN is trained using a back-propagation algorithm with momentum.[24] The algorithm requires two parameters: the learning rate and momentum term. The momentum term was fixed at 0.71 and the learning rate was fixed at 0.08. The network was trained five times starting each time with a randomly chosen set of weights. As widely known, during the training, the weights and the biases of the network are iteratively adjusted to minimise the network error function. The network error used in this work is the mean square error correspondent to the training set elements. This error is monitored during the training process and will normally decrease during the training. However, when the network becomes excessively specialised in reproducing the training data, the early stopping error will typically begin to rise.[25] When the early stopping error increases for a specified number of iterations, the training is stopped, and the weights and biases at the minimum early stopping error are returned. Optimal training was achieved in 74 epochs. In Figure 5 the ANN performance is depicted in terms of linear regression between dataset (split into the typical subsets training, validation and testing). As already stated, once trained the ANN accepts any vector P_j as input and computes instantly the correspondent neural network output vector, that is, the corresponding value l_j.

The ANN has been tested with 20 new sets of potentials. The average difference between estimated and actual l_i values was equal to 0.057 m with a variance equal to 0.001. Consequently, based on experimental tests, it can be stated that the results obtainable from the ANN are comparable to the ones derived from the simulation.

It is worth noting again that the main aim in devising the ANN described above is not to overcome the performance of the trajectory simulation algorithm, neither to replace it. It is, rather, a method to artificially and considerably increase the amount of experimental data for applying optimization algorithms aimed at determining the optimal potential parameters. In fact, since a single simulation using the ANN is performed in less than 0.05 s with commercial hardware consisting of an Intel Core i7-2860QM processor with 24 GB RAM, it is plausible to test a huge number of different parameter values.

Accordingly, the main idea is to solve the following optimization problem.[26]

Given:

1. a set of vectors P_k obtained by varying k times and one by one the parameters within their given range with a given step; in Table 3 the steps used for each parameter are listed. In this work, since four states are used for each of the 10 parameters, the number of the k tested solutions is equal to $4^{10} = 1,048,5761$;
2. a set of l_k outputs obtained by simulating the ANN using the vectors P_k;
3. the absolute difference value δ_k between the l_k value and the desired optimal position of the transported object l_{opt} defined as follows

$$l_{\text{opt}} = \frac{d_{\text{obs}}, +w_{\text{obj}}}{2} + \epsilon \tag{22}$$

$$\delta_k = |l_k - l_{\text{opt}}| \tag{23}$$

where d_{obs} is the obstacle diameter, w_{obj} is the width of the transported object and ϵ is a precautionary distance (between such an object and the obstacle) to be maintained during the object transportation phase along the desired trajectory.

Find:

- the vector P_{opt} allowing the minimum value $\delta_{\text{opt}} \in \{\delta_k\}$ to be obtained.

This optimization problem is solved using a brute force algorithm, that is, performing an exhaustive search of the solution domain δ_k to find the input P_{opt} achieving the

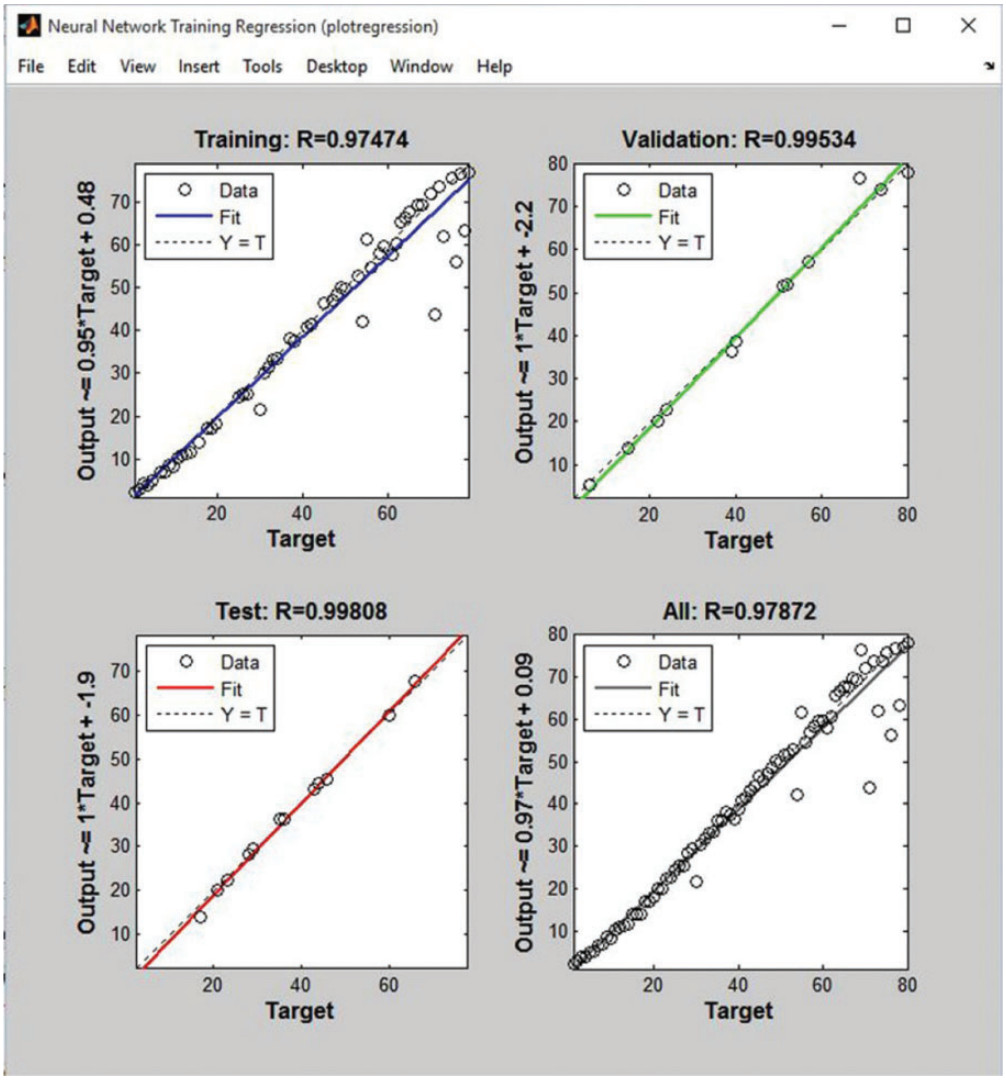

Figure 5. ANN performance.

absolute minimum value δ_{opt}. Since the overall number of simulations carried out using the ANN is, as already stated, $k = 4^{10}$, the computational time for determining the whole set of distances is equal to approximately 14 hours and 33 minutes when the above hardware is used.

Finally, simulating the trajectory of a swarm transporting an object whose width $w_{\text{obj}} = 2$ m, supposed to avoid an obstacle with a diameter of 2 m and using a 0.6 m value for ε (i.e. $l_{\text{opt}} = 3.6$ m), the retrieved optimal set P_{opt} is the following

$$\vec{P}_{\text{opt}} = (5, 10, 0.1, 2, 1.5, 0.8, 99.5, 100.5, 16, 10) \quad (24)$$

Such a set provides $\delta_{\text{opt}} = 0.23$ m.

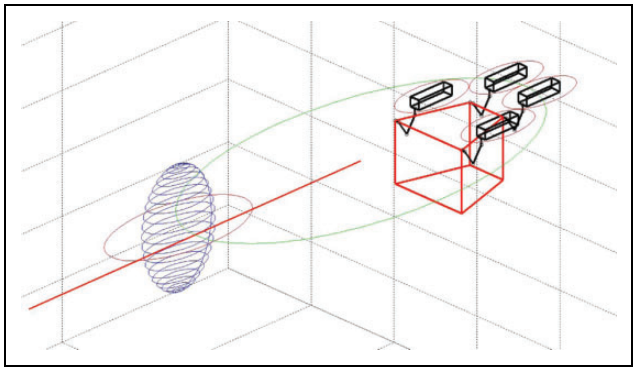

Figure 6. Zoom on the initial conditions of the intervention-autonomous underwater vehicles swarm.

Numerical simulations and results

In this section the results of the numerical simulations are analysed. The objective of this analysis is to test the proposed cooperative strategy for a swarm of I-AUVs, highlighting its advantages and drawbacks. The simulated tasks are referred to the potential functions shown in the

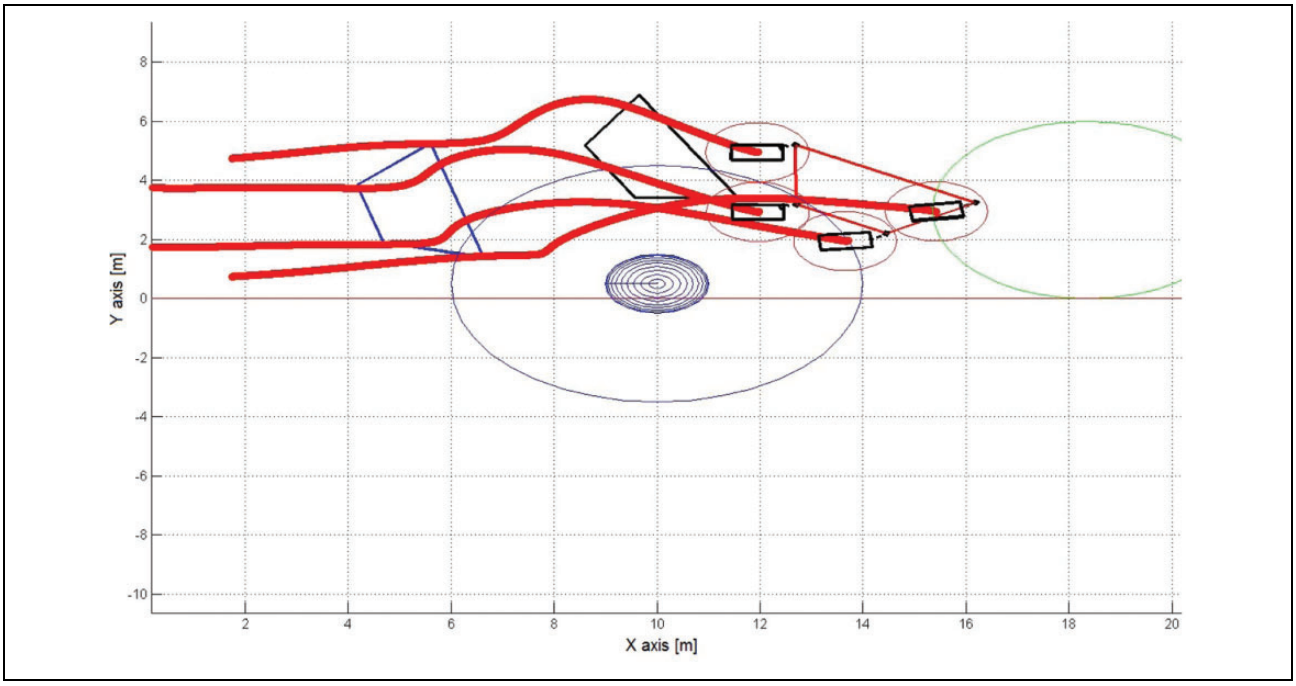

Figure 7. Trajectories of the intervention-autonomous underwater vehicles swarm during the manipulation task: XY plane.

section 'A new strategy for I-AUVs swarms performing cooperative mobile manipulation'. The sum of all these contributions determines the I-AUVs swarm trajectory. The analysed task is a classical transportation task in which the swarm is composed of four I-AUVs with six DOFs. Each vehicle has a single robotic arm with seven DOFs and a gripper that is (for hypothesis) rigidly connected with the object. In this simulation the approaching phase to the object is neglected. The simulation environment is Matlab-Simulink where the I-AUVs are modelled using the multi-body approach explained in the section 'Artificial Neural Network for parameter optimization'. The integrator used is the fixed-step differential equation implemented by Dormand-Prince [5], with a step size of $\Delta t = 1e^{-4}$ s.

In this part, the preliminary results of the cooperative manipulation with obstacle avoidance are shown. The cooperative mobile manipulation is performed by four I-AUVs placed at the four corners of the object. The trajectory is calculated by the sum of all contributions (vehicle–vehicle, vehicle–object, vehicle–environment potentials). The obstacle is modelled as a sphere placed along the desired trajectory of the swarm.

In Figure 6, the initial positions of the vehicles are represented; in addition, the influence of the potentials is shown (the red circle is the vehicle–object potential and the green circle is the vehicle–vehicle one). The red line is the desired trajectory of the swarm imposed by the ROSV (support surface vehicle).

Finally, Figure 7 represents the final condition of the I-AUVs swarm, after the obstacle avoidance phase in which the object is carried by the swarm; the trajectory of the vehicles in the XY plane is shown. The results are

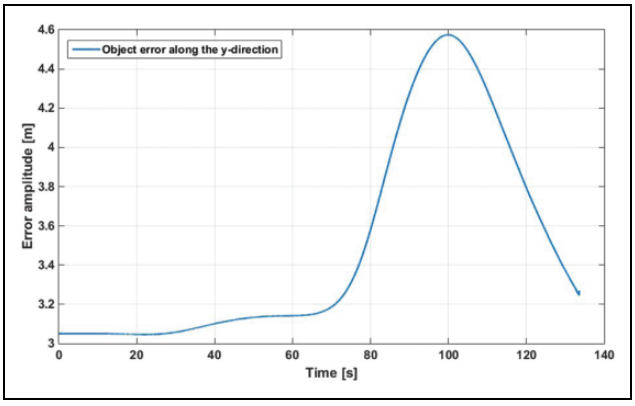

Figure 8. Tracking error of the object with respect (y-coordinate).

encouraging because the dynamical behaviours of the I-AUVs are very smooth. The vehicles have not yet reached the swarm formation (the green circle); in addition, it is possible to evaluate the behaviour of the manipulated object that avoids the obstacle. There are three different time instants shown on this figure: the blue object is at the beginning of the obstacle avoidance phase, the black object is at the maximum effect of the V_{v-e} potential that forces the object to avoid the obstacle and, finally, the red object at the final situation of the swarm.

In Figure 8, the tracking error of the object with respect to the desired straight trajectory is shown. The error is highlighted only in terms of y-direction because the potentials work mainly in that direction in this task. As depicted, the error is initially zero but, when the swarm arrives near the obstacle, I-AUVs begin to avoid the obstacle, changing

their trajectories and the trajectory of the object. After the obstacle avoidance phase, the swarm comes back to follow the ideal trajectory of the swarm. It is worth noting that the slope and the amplitude of the obstacle avoidance phase mainly depend on the potential parameters. This simulation represents a particular case of cooperative mobile manipulation, but different testing conditions have been assessed. In addition, during this task, both the distance estimation algorithm and the cooperative control strategy have shown a promising behaviour. The localization algorithm worked well and should be tested by introducing some realistic effects like delays, loss of information, etc. The cooperative control strategy based on the latter algorithm has shown a strong dependence on the amplitude of the potential parameters. A more deep analysis of the correlations among these parameters and the effects on the dynamical behaviour of the vehicles could clarify the best solution for the potential parameter tuning.

Conclusions and further developments

The study of cooperative manipulation strategies of I-AUVs represents a more complex field of application, compared with the terrestrial or aerial ones, mainly due to different technological problems, e.g. localization and communication in an underwater environment. In this article, an innovative decentralized approach for cooperative mobile manipulation of I-AUVs based on the potential field method has been presented; the potential field parameters have been optimized through a suitable and trained ANN. The control architecture is developed to manage in parallel the coordination of the swarm, the guidance and navigation of I-AUVs and the manipulation tasks within a unique control structure. The future developments planned for this research activity will be the implementation in the model of more-complex functions describing sensor and actuator performance, regarding optical and acoustic devices, the introduction of different constraints between objects and the grippers and the testing of the proposed control architecture based on the potential field method, with the underwater vehicles built by the authors' laboratory.

Declaration of conflicting interests

The author(s) declared no potential conflicts of interest with respect to the research, authorship, and/or publication of this article.

Funding

The author(s) received no financial support for the research, authorship, and/or publication of this article.

References

1. Joordens MA and Jamshidi M. Underwater swarm robotics consensus control. *Syst Man Cybern, 2009. SMC 2009. IEEE International Conference on*, San Antonio, TX, USA, 11–14 October 2009, pp.3163–3168. IEEE.
2. Champion BT and Joordens MA. Underwater swarm robotics review. In: *10th System of Systems Engineering Conference SoSE)*, San Antonio, TX - USA, 17–20 May 2015, pp.111–116. IEEE.
3. Siciliano B and Khatib O. *Handbook of robotics*. Naples, Italy and Stanford, CA: Springer Handbooks, 2008.
4. Antonelli G. *Underwater robots,* Springer Tracts in Advanced Robotics. 2nd ed. Heidelberg: Springer-Verlag, 2006.
5. Simetti E, Casalino G, Torelli S, et al. Floating underwater manipulation: Developed control methodology and experimental validation within the TRIDENT Project. *J Field Rob* 2014; 31: 364–385.
6. Hirata Y, Kume Y, Sawada T, et al. Handling of an object by multiple mobile manipulators in coordination based on casterlike dynamics. In: *IEEE international conference on robotics and automation* (ed Lee G), New Orleans, LA, USA, 26 April–1 May 2004, pp.807–812. IEEE.
7. Abreu PC, et al. Cooperative formation control in the scope of the EC MORPH project: Theory and experiments. In: *OCEANS*, Genova, Genoa, 18–21 May 2015, pp.1–7. IEEE.
8. Häusler AJ, Saccon A, Aguiar AP, et al. Energy-optimal motion planning for multiple robotic vehicles with collision avoidance. *IEEE Transactions on Control Systems Technology* 2016; 24(3): 867–883.
9. Tanner HG, Loizou S and Kyriakopoulos KJ. Nonholonomic navigation and control of cooperating mobile manipulators. *IEEE Trans Robot Autom* 2003; 19: 53–64.
10. Bullo F, Cortes J and Martinez S. *Distributed control of robotic networks.* Princeton, New Jersey: Princeton University Press, 2008.
11. Olfati-Saber R, Fax JA and Murray RM. Consensus and cooperation in networked multi-agent systems. *Proc IEEE* 2007; 95: 215–233.
12. Bahr A, Leonard JJ and Fallon MF. Cooperative localization for autonomous underwater vehicles. *The International Journal of Robotics Research* 2009; 28(6): 714–728.
13. Antonelli G, Caccavale F, Chiaverini S, et al. Tracking control for underwater vehicle manipulator systems with velocity estimation. *IEEE J Oceanic Eng* 2000; 25: 399–413.
14. Fossen TI. *Guidance, navigation and control of ocean vehicles. 1st ed*. Chichester, UK: John Wiley&Sons, 1994.
15. Sugar TG and Kumar V. Vehicle/arm coordination and multiple mobile manipulator. *IEEE Trans Rob Autom* 2002; 18: 94–103.
16. Conti R, Meli E, Ridolfi1 A, et al. An innovative decentralized strategy for I-AUVs cooperative manipulation tasks. *Robotics and Autonomous Systems* 2015; 72: 261–276.
17. Allotta B, Costanzi R, Meli E, et al. Cooperative localization of a team of AUVs by a tetrahedral configuration. *Robotics and Autonomous Systems* 2014; 62(8): 1228–1237.
18. Nikolay B, Vadim B, Yaniss T, et al. Modeling of the Manipulation Operationon Sunken Submarines for the Underwater RemotelyOperated Vehicle. *International Journal of Modeling and Optimization* 2012; 2(5): 579.

19. Polak E. *Optimization: Algorithms and consistent approximations*. Vol. 124. New York: Springer Science and Business Media, 2012.
20. Furferi R and Carfagni M. Colour mixing modelling and simulation: Optimization of colour recipe for carded fibres. *Modell Simul Eng* 2010; 487678.
21. Box GE, Hunter WG and Hunter JS. *Statistics for experimenters: Design, innovation, and discovery*. 2nd ed. Hoboken, New Jersey: Wiley, 2005.
22. Hong-Te S, et al. Integrating neural networks with first principles models for dynamic modeling. In: Balchen JG, Gilles ED, Waller KV and Rawlings JB (eds) *Dynamics and control of chemical reactors, distillation columns and batch processes*, Maryland, USA, 26–29 April 1992. Oxford, England: Elsevier, 2014.
23. Furferi R, Governi L and Volpe Y. Neural network based classification of car seat fabrics. *Int J Math Models Methods Appl Sci* 2011; 5: 696–703.
24. Phansalkar VV and Sastry PS. Analysis of the back-propagation algorithm with momentum. *IEEE Trans Neural Networks* 1994; 5: 505–506.
25. Furferi R, Governi L and Volpe Y. Modeling and simulation of an innovative fabric coating process using artificial neural networks. *Text Res J* 2012; 82: 1282–1294.
26. Governi L, Furferi R and Volpe Y. A genetic algorithms-based procedure for automatic tolerance allocation integrated in a commercial variation analysis software. *J Artif Intell* 2012; 5: 99–112.